Article

Not peer-reviewed version

Development of a Multilayer Transdermal Patch Platform Based on Electrospun Nanofibers for the Delivery of Caffeine

Jorge Teno , Zoran Evtoski , Cristina Prieto , Jose Lagaron *

Posted Date: 31 March 2025

doi: 10.20944/preprints202503.2249.v1

Keywords: electrospinning; transdermal delivery

Article

Development of a Multilayer Transdermal Patch Platform Based on Electrospun Nanofibers for the Delivery of Caffeine

Jorge Teno [1], Zoran Evtoski [2], Cristina Prieto [2] and Jose M. Lagaron [2,*]

[1] R&D Department, Bionanopharma S.L., Calle Algepser 65 nave 3, 46980 Paterna, Valencia, Spain

[2] Novel Materials and Nanotechnology Group, Spanish Council for Scientific Research (CSIC), IATA, Calle Catedrático Agustín Escardino Benlloch 7, 46980 Paterna, Valencia, Spain

* Correspondence: author: lagaron@iata.csic.es (J.M. Lagaron)

Abstract: The work presented herein focuses on the development and characterization of a transdermal caffeine platform fabricated from ultrathin micro- and submicron fibers produced via electrospinning. The formulations incorporated caffeine encapsulated in a polyethylene oxide (PEO) matrix, combined with various permeation enhancers. A backing layer made of annealed electrospun polycaprolactone (PCL) facilitated the lamination of the two layers to form the final patch. Comprehensive characterization was conducted, utilizing scanning electron microscopy (SEM) to assess fiber morphology, attenuated total reflectance Fourier transform infrared spectroscopy (ATR-FTIR) for chemical detection and stability of the caffeine, and differential scanning calorimetry (DSC) along with wide-angle X-ray scattering (WAXS) to analyze the physical state of caffeine within the fibers of the active layer. Additionally, Franz cell permeation studies were performed using both synthetic membranes (Strat-M) and ex vivo human stratum corneum (SC) to evaluate and model the permeation kinetics. These experiments demonstrated the significant role of enhancers in modulating caffeine permeation rates from the patch, achieving permeation rates of up to 0.73 mg/cm² within 24 hours. This work highlights the potential of the electro-hydrodynamic processing technology to develop innovative transdermal delivery systems for drugs, offering a promising strategy for enhanced efficacy and innovative therapeutic direct plasma administration.

Keywords: electrospinning; transdermal delivery

1. Introduction

Transdermal drug delivery systems (TDDS), commonly referred to as "patches," are an alternative to oral drug administration and hypodermic injections. TDDS offer several advantages over other administration routes, including bypassing first-pass metabolism, ease of self-administration, reduced dosing frequency, and minimized gastrointestinal side effects. Despite these benefits, delivering most drug molecules via the transdermal route remains one of the greatest challenges in TDDS development. The primary barrier to transdermal drug delivery (TDD) is the stratum corneum (SC), the outermost layer of the skin. The SC has a dense cellular architecture that significantly limits percutaneous absorption. Composed of non-polar lipids and neutral keratin proteins, the SC requires drug molecules to have adequate solubility in both water and oil to permeate through the skin effectively [1,2] Drug molecules can penetrate the skin via three main pathways: (i) intracellular diffusion across SC corneocytes, (ii) penetration through the SC's intracellular lipid spaces, and (iii) penetration through skin appendages. Among these, the intracellular lipid domain of the SC is considered the principal pathway for drug penetration by the scientific community. There are three different routes for percutaneous penetration of the drug molecules: intracellular diffusion across the SC corneocytes, penetration through the SC intracellular lipid spaces, and penetration through skin appendages. Among these, the intracellular lipid domain

 doi:10.20944/preprints202503.2249.v1

of the SC is the principal pathway for drug molecules to penetrate through the skin according to scientific community, [3,4].

Chemical strategies to reduce the effect of the barrier include the use of penetration enhancers. Transdermal enhancers are introduced into patches to overcome the excellent barrier function of the SC by temporary weakening the skin barrier. They are effective in increasing skin permeation rates and improving skin delivery of topically active drugs, reducing the permeability barrier without causing significant damage to cells. Enhancers can also modify the properties of the formulation to promote drug delivery [5–7]. They can be classified according to their chemical composition in different groups such as alcohols, fatty acids, glycols, or surfactants among others [8] . Depending on the chemical properties and the interactions between drugs and enhancer, the choice of the appropriate enhancer could anticipate the mechanism of action of the drug and improve the drug permeation. A wide range of enhancers shows potent permeation-enhancing effects, nevertheless they are drug-specific, and they do not have the same effect with all the drugs. For example, Span 80 increase the permeation of diclofenac and olanzapine by 4.4 and 1.6 folds, respectively, but it reduces the permeation of flurbiprofen by 0.8 folds [9,10] . Xu et al. studied the specificity of enhancement effects in relation to polyglyceryl-3-dioleate (POCC) on ten drugs. They found that drugs with low polar surface area value exhibited a high partition after the addition of POCC. Furthermore, the permeation of drugs with low polar surface area and polarizability was enhanced more significantly by POCC, which was illustrated by the interactions among drugs, POCC and skin lipids . [11]

Drug-in-adhesive patches are the most commonly used system for combining drugs and enhancers in an adhesive matrix that remains in direct contact with the skin. However, these systems often face challenges, such limited drug loading, relatively low permeation, limited drug choices or compatibility issues, skin irritation, etc. [12]. Addressing some or all of these disadvantages often involves exploring alternative technologies, such as multilayer systems [13,14], microneedles [15,16] or electrospun nanofibers to enhance drug delivery efficiency and expand the range of deliverable therapeutics [17,18]

In recent years, the electrospinning technique has gained attention as a promising method to increase the bioavailability of active ingredients. Electrospinning is one of the simplest and most versatile methods for producing ultrathin fibers, so-called electrospun nanofibers, with applications across a broad range of materials. Notably, the rapid solidification process of electrospun nanofibers and the interactions between the drug and the fiber matrix have been shown to improve drug dispersion [18,19]. The technique allows the use of a wide variety of polymers, making it adaptable for diverse drug formulations and therapeutic applications. Moreover, the high surface area of electrospun fibers enhances drug dispersion within the patch, potentially enabling more consistent and controlled drug delivery. Electrospinning also offers the potential to incorporate drugs with poor solubility into nanofibers, thereby improving their solubility and bioavailability. Additionally, this technique accommodates a wide range of drug types, including small molecules, peptides, and proteins, making it a versatile platform for drug encapsulation.

Besides, electrospinning can protect drug from degradation or premature release, increasing their stability in the delivery system [20–22].

Caffeine which has the name of chemical compound 1,3,7- trimethylxanthine is being used in some applications. Caffeine provides Caffeine is utilized in the pharmaceutical industry for various purposes. Some of the most common applications of caffeine in medications include: analgesia, caffeine is used as an adjunct in analgesics to enhance their efficacy [23], central nervous system (CNS) stimulant [24], dermatological applications [25], etc.. Caffeine applied topically is available in the form of creams and lotions, primarily because of its diverse effects on the skin [26]. It is also recognized for its potential to slow down the skin aging process by offering protection against ultraviolet light, absorbing UV radiation, and reducing the risk of skin cancer. Additionally, caffeine is an active ingredient in anti-cellulite formulations, known for its robust antioxidant properties. It can enhance blood microcirculation within the skin and promote hair growth by inhibiting the activity of the enzyme 5-α-reductase [27]. Caffeine, being considered a hydrophilic drug with a LogP

 doi:10.20944/preprints202503.2249.v1

of -0.07, has also being used as a model drug for active principle ingredients with low skin permeability and low water solubility [28]. Caffeine together with other actives have been previously encapsulated in monolayers to be used as potential oral dispersable films in other electrospun fiber materials such as PVOH and PVP [28,29].

The aim of this seminal study was to develop a multilayer electrospun patch platform from pharma grade polymeric materials to evaluate caffeine transdermal drug delivery. Hydrophilic polyethylene oxide (PEO) was used as a model polymer to provide skin adhesion and homogeneous drug delivery, and the bipolymer polycaprolactone (PCL) was selected as the backing hydrophobic layer. The electrospun nanofibers were characterized using scanning electron microscopy (SEM), attenuated total reflectance Fourier-transform infrared spectroscopy (ATR-FTIR), and wide-angle X-ray scattering (WAXS). Drug permeation was analyzed using a Franz diffusion cell tool, initially with a multilayer synthetic membrane, followed by testing on human biopsy stratum corneum membranes to assess ex-vivo permeation and permeation kinetics of the optimal candidate.

2. Materials and Methods

2.1. Materials

Caffeine (powder, Reagent Plus®), polyethylene glycol (PEG, MW400), oleic acid (OA, technical grade 90%) and chloroform (ACS reagent, ≥99.8%) were purchased from Sigma-Aldrich (Madrid, Spain). Methanol (MeOH) and propylene glycol (PG, pharma grade) was supplied by Panreac Química S.L.U. (Castellar del Vallès, Barcelona). Polyethylene oxide (PEO, Mw 200000 Da) was purchased from the Dow Chemical Company (Montgomeryville, PA, USA) and Poly-ε-caprolactone (PCL, Resomer C212) supplied by Evonik Industries (Essen, Germany), Eucalyptus Globulus Leaf Oil (80-85% of 1,8-cineole) was supplied by Gran Velada. Dulbecco's Phosphate-Buffered Saline (DPBS) solution without calcium and magnesium ions was purchased from Thermo Fisher Scientific. All the polymers and reagents were used as received without further purification.

2.2. Solution Preparation

The solutions of the active adhesive layer were prepared by first dissolving the polymer in the appropriate solvent. Caffeine and the corresponding enhancers were then added to the solution under continuous stirring at room temperature. Caffeine is known to be soluble in a chloroform/methanol solvent mixture. In all cases, with or without enhancers, stable and transparent solutions were obtained, with no precipitation observed in the injector during and after the electrospinning process. The developed solutions are gathered in **Table 1**.

 doi:10.20944/preprints202503.2249.v1

Table 1. Composition of PEO-caffeine solutions.

Sample ID	Ratio Polymer/API/Enhancer (w/w)	Solvents and ratio (w/w)
PEO_CAF	80/20	Chloroform/MeOH (80:20)
PEO_CAF_OA	70/20/10	
PEO_CAF_PEG	64/20/16	
PEO_CAF_PG_OA	56/20/14/10	
PEO_CAF_PEG_OA	56/20/14/10	
PEO_CAF_PEG_EUC	60/20/15/5	

2.3. Electrospinning

Electrospinning process was carried out in a Fluidnatek™ LE-100 equipped with a 5-multi-emitter injector system from Bioinicia S.L. (Valencia, Spain) and an air-conditioned unit system. **Table 2** shows the electrospinning parameters used for each solution. The environmental conditions were kept at 30°C and 25 % relative humidity (RH) for all the electrospinning processes.

Table 2. Electrospinning parameters of the PEO containing caffeine solutions with different enhancers, and the backing layer (BL).

Sample ID	Flow-rate (mL/h)	Voltage V+/V- (kV)	Needle-to collector distance (cm)
PEO_CAF	10	20/-5	20
PEO_CAF_OA	10	20/-10	20
PEO_CAF_PEG	10	20/-10	20
PEO_CAF_PG_OA	10	20/-10	20
PEO_CAF_PEG_OA	10	20/-10	20
PEO_CAF_PEG_EUC	10	20/-10	20
BL (PCL)	20	15/-2	15

For this study, bi-layer patches were prepared as follows. First, the reservoir layer was made of electrospun PEO fibres containing caffeine and the correspondent enhancers (**Figure 1a)**. Then, the hydrophobic backing layer (BL) made of electrospun PCL fibres was electrospun separately (**Figure 1b)** and laminated to the previously prepared material using a hot press (Carver 4122, Wabash, IN, USA) for 20 s without pressure to assemble the whole multilayer patch (**Figure 1c, d)**. The surface density was optimized at 10 g/m^2 for the backing layer and 70 g/m^2 for the active layer.

 doi:10.20944/preprints202503.2249.v1

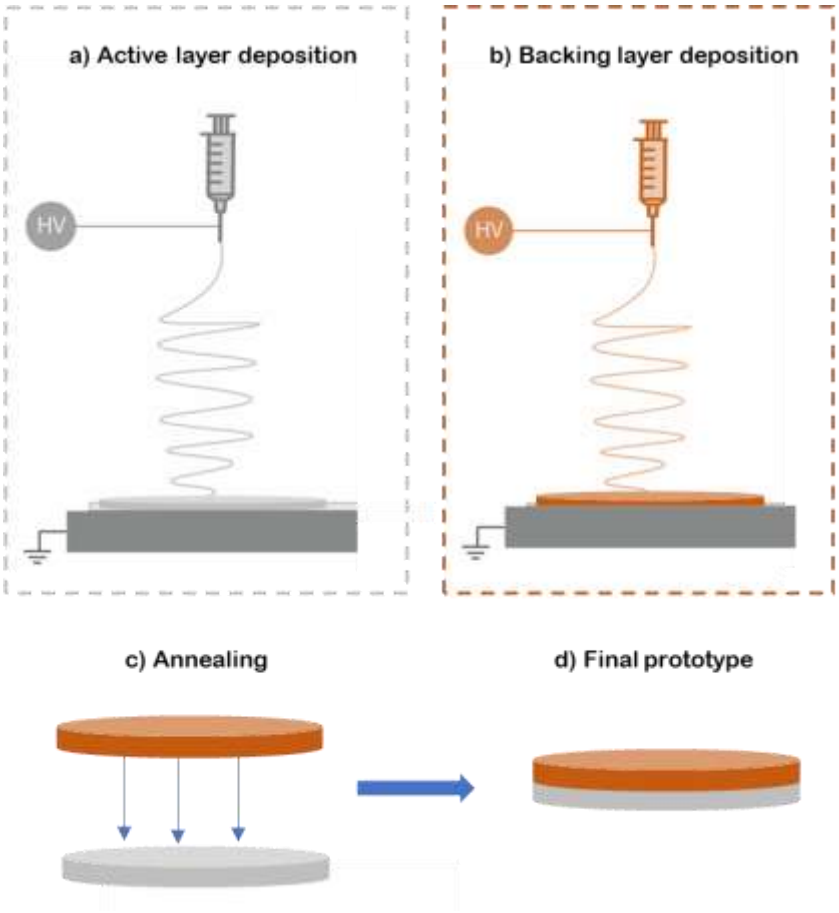

Figure 1. Diagram of the formulation of the multilayer patch. **a)** electrospinning of the active layer (grey); **b)** backing layer electrospun separately from the previous layers (orange); **c)** Lamination at low temperature by annealing of the backing layer to the reservoir layer; **d)** final bi-layer patch prototype.

2.4. Human Skin Sample Preparation

Skin biopsy specimens from two healthy volunteers, a 39-year-old white skin with hair follicles man and a 68-year-old white skin woman, stored at -80°C, were provided by the Biobank of the Valencia Region, Spain. Briefly, the full-thickness skin was sealed in sterile plastic bags and frozen at -80°C within 24 hours of removal to be used within a month period. Before preparation, the skin was thawed to room temperature, and any excess fat was carefully removed. The subcutaneous tissue was meticulously excised using an aseptic scalpel, and the skin was cut into pieces according to the requirements of the permeation experiments. The skin pieces were immersed in preheated Dulbecco's phosphate-buffered saline (DPBS) at 60°C for 45–60 seconds. The excess DPBS was removed, and the stratum corneum layer was gently peeled away from the biopsy using sterile forceps. The SC is considered the outer most hydrophobic barrier layer in the skin.

2.5. Characterization

2.5.1. Fibre Morphology (SEM)

The fibre morphology of the different produced patches was analyzed by scanning electron microscopy (SEM) using a Phenom XL G2 Desktop microscope (Thermo Fisher Scientific, Waltham, MA, USA) with an electron beam acceleration of 5 kV. Average fibre diameter based on at least 100 fibres was determined using a Phenom ProSuite Software on SEM images.

 doi:10.20944/preprints202503.2249.v1

2.5.2. In-Vitro Release Assessment of Caffeine Patches Using Franz Diffusion Cell

The release experiments were performed using a Franz diffusion cell equipment at 35ºC with an effective diffusion area of 1 cm^2. In a first experiment, a polyether sulfone membrane Strat-M® was placed between the donor and receptor chambers of the Franz diffusion cell. The permeation experiments with such synthetic membrane were done in triplicate. To preserve the temperature of the receptor solution at 35ºC, a water jacket was connected to a water bath with continuous recirculating water. Patches were cut into 1 cm^2 effective surface, and placed on top of Strat-M membrane, then the assembly was mounted on the receptor chamber containing 8.0mL of PBS buffer solution (pH 7.4). The upper and lower part of the Franz cell were sealed with parafilm and fastened together by means of a clamp. In-vitro caffeine permeation was monitored for different lengths of time: 1, 3, 6, 8 and 24h. Certain amount of the solution, 0.5 mL, was withdrawn from the receptor chamber and then replaced with the same volume of PBS solution (pH 7.4) to keep the sinking volume constant throughout the analysis. The caffeine concentration was determined using a HPLC Acquity® TQD (Waters) equipped a C18 column (BEH, 1.7 µm, Waters) and a mass detector.

The patch displaying the best results of caffeine permeation using Strat-M was further evaluated using two ex-vivo human skin specimens from the two donors. Each specimen was mounted onto the Franz diffusion cell with the epidermis facing downward and the stratum corneum side in contact with the patch under investigation.

Fourier transform infrared (FTIR)

The presence of the caffeine in the polymer matrix was evaluated with a Fourier transformed infrared spectroscopy and measured with a Bruker Tensor 37 FT-IR Spectrometer (Bruker, Ettlingen, Germany) coupled with the attenuated total reflectance (ATR) sampling accessory Golden Gate (Specac Ltd., Orpington, UK). Spectra were collected from the average of 64 scans in the range of 4000-600 cm^{-1}, with a resolution of 4 cm^{-1}.

2.5.3. Differential Scanning Calorimetry (DSC)

The electrospun fibres were studied by differential scanning calorimetry (DSC) on a DSC-8000 analyzer equipped with a cooling accessory Intracooler 2 from PerkinElmer, Inc. (Waltham, MA, USA). Approximately 3 mg of each sample were placed in standard aluminum pan and heated from 0 to 300 ºC and at a rate of 10 °C/min using a nitrogen flow of 20 mL/min as the sweeping gas.

2.5.4. Wide-Angle X-Ray Scattering (WAXS)

Samples were analyzed using a Bruker AXS D4 Endeavor diffractometer (Bruker, Ettlingen, Germany). Samples were scanned by wide-angle X-ray scattering at room temperature in reflection mode, using incident Cu K-alpha radiation (Cu Kα = 1.54 Å) while the generator was set up at 40 kV and 40 mA. The data were collected over a range of scattering angles (2θ) in the 5–40° range. To estimate the average crystallite size of caffeine the Scherrer equation was used:

$$D = \frac{K\,\lambda}{\beta\,\cos\theta} \quad (1)$$

where, D is the crystallite size, K is shape factor, λ is the XRD radiation wavelength, β is the full width at half maximum of the peak in radian.

2.5.5. Kinetic Modelling of Ex-Vivo Human Skin Permeation

To analyze the kinetics of the *in vitro* drug release behavior of the patch, semi-empirical mathematical models were fitted to the caffeine permeation curve through human skin. The model of Korsmeyer-Peppas was used to fit the experimental data, since no burst release was observed that would have justified the use of other modified models such as the Ritger-Peppas.

The Korsmeyer-Peppas model it is mathematically described as follows:

$$Q = Kt^n \quad (2)$$

 doi:10.20944/preprints202503.2249.v1

where Q is the amount of drug released over time t, K is the constant of incorporation of structural modifications and geometrical characteristics of the system (also considered the release velocity constant), n is the release exponent (which depends on the type of drug polydispersity, geometry, and transport) in function of time t. Depending on the release exponent, diffusional release mechanisms were classified as; $n<0.5$ pseudo-Fickian diffusional behavior, $n = 0.5$ Fickian diffusion, $0.5<n<1$ non-Fickian diffusion, $n = 1$ case II transport (zero order release), and n>1 super case II transport [30].

3. Results and Discussion

3.1. Fibre Morphology (SEM) of the Active Layer

The fibre morphology of the different PEO/caffeine patches was analyzed by SEM. On the one hand, the fibres without enhancer or containing one enhancer in its formulation displayed similar morphology. These fibres display a flattened morphology (See Figure 2). On the other hand, the fibres containing two enhancers displayed a rounded morphology. This difference could be attributed to the solvent evaporation rate during the electrospinning process, when the solvent was evaporated more rapidly the fibres collapse leading to a planar morphology. If solvent evaporates more slowly the fibres could keep a round morphology. In is interesting to note that some caffeine like needles crystals were seen at the fiber surface for some of the samples with the exception of the samples e) and f) containing polyethylene glycol and oleic acid and polyethylene glycol and eucalyptol mixtures, respectively [31]. Regarding the fibre size corresponding to the various patches with different enhancers are summarized in Table 3. The fibres containing PEG and OA as enhancers displayed smaller diameter than the rest of fibres

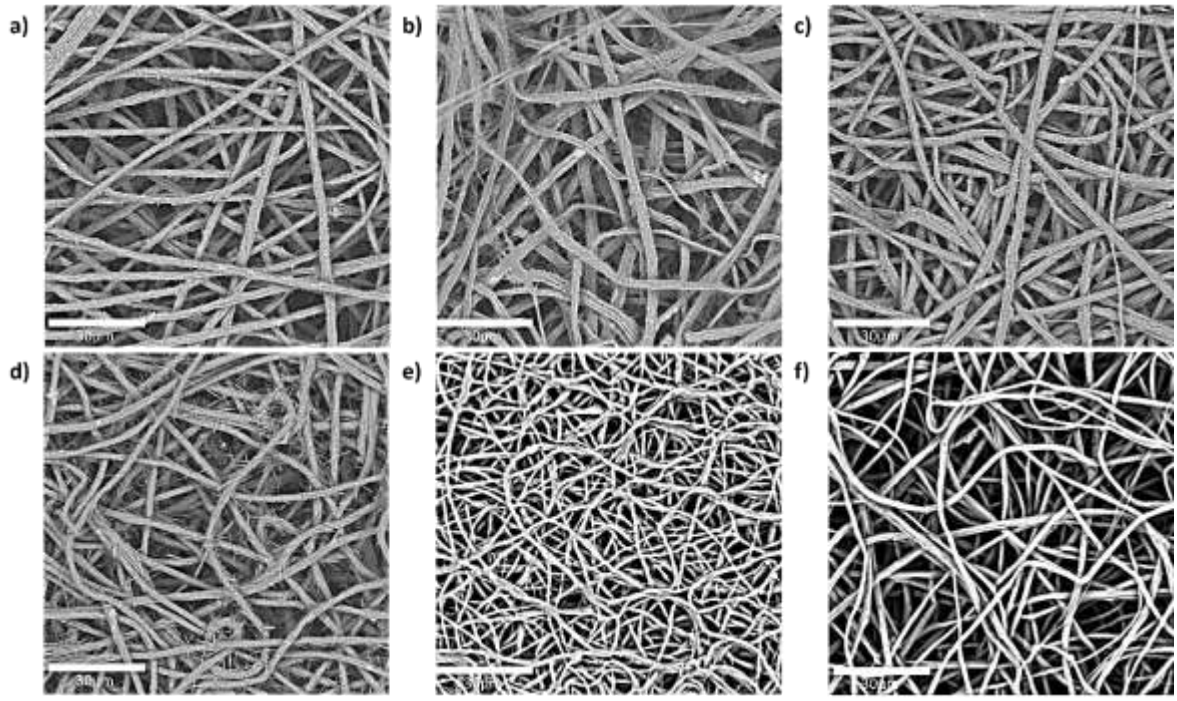

Figure 2. SEM images of PEO/caffeine patches with different enhancers a) without enhancer; b) oleic acid; c) polyethylene glycol; d) propylene glycol and oleic acid; e) polyethylene glycol and oleic acid; and f) polyethylene glycol and eucalyptol.

 doi:10.20944/preprints202503.2249.v1

Table 3. Fibre size of PEO/caffeine patches with the different enhancers and presence of caffeine at the fibre surface.

Sample ID	Fibre size (μm)	Caffeine at fibre surface
PEO_CAF	2.1 ± 0.5	Yes
PEO_CAF_OA	2.8 ± 0.4	Yes
PEO_CAF_PEG	2.3 ± 0.4	Yes
PEO_CAF_PG_OA	2.2 ± 0.4	Yes
PEO_CAF_PEG_OA	1.1 ± 0.2	No
PEO_CAF_PEG_EUC	1.7 ± 0.2	No

3.2. Effect of the Enhancer on the Permeation of Caffeine

Figure 3 and Table 4 gather the permeation data through the Strat-M membrane of caffeine-loaded PEO electrospun patches with different enhancers. As it can be observed, the enhancer has a strong influence on caffeine permeation. The patches containing PEG_OA, PEG_EUC and PEG displayed higher caffeine permeability than patches containing the other enhancers. The compatibility of the enhancers with caffeine, from most soluble to least soluble, is as follows: PEG, PEG_OA mixture, PEG_EUC mixture, PG, and PG_OA mixture and OA. Interestingly, the patch containing the enhancer mixture PEG_OA displayed the highest caffeine permeability in 24 hours, around 36 ± 1%. This result is in good agreement with observations of this mixture being ranked as highly compatible with caffeine and the fibers not showing detectable traces of caffeine crystals over the fiber surface. In addition, PEG is considered as a non-ionic surfactant as it can potentially interact with biological membranes, especially skin, causing an increase in their permeability and the transmembrane transport of solutes which together with OA could synergistically reduce the diffusional resistance of the skin by interacting with the lipid matrix, since OA has been reported to increase lipid fluidity [8,32] . In view of the results, the patch PEO_CAF_PEG_OA, was selected to perform additional permeation test through human SC biopsies.

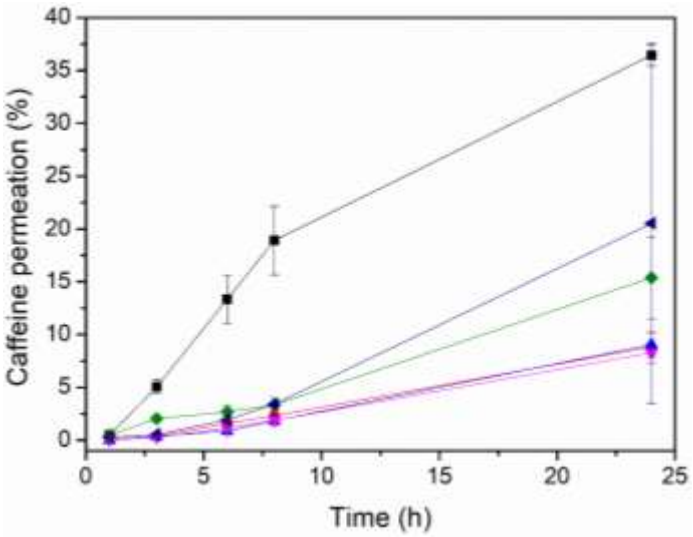

Figure 3. Caffeine permeation in μg/cm² of the PEO/caffeine patches with different enhancers: without enhancer, oleic acid, polyethylene glycol, polyethylene glycol and oleic acid, propylene glycol and oleic acid, and polyethylene glycol and eucalyptol oil.

 doi:10.20944/preprints202503.2249.v1

Table 4. Initial caffeine in the patch and the corresponding permeated caffeine in 24 hours.

Sample ID	Initial Caffeine (mg/cm²)	Permeated caffeine (mg/cm²)
PEO_CAF	1.33	0.15 ± 0.01
PEO_CAF_OA	1.87	0.17 ± 0.02
PEO_CAF_PEG	1.85	0.31 ± 0.08
PEO_CAF_PG_OA	1.95	0.17 ± 0.04
PEO_CAF_PEG_OA	2.02	0.73 ± 0.02
PEO_CAF_PEG_EUC	1.69	0.41 ± 0.34

3.3. Fourier Transform Infrared (FTIR)

The FTIR spectra of pure caffeine, the placebo layer and the active layer are shown in **Figure 4**. The FTIR spectrum of caffeine powder shows two peaks at 3110 cm^{-1} and 2955cm^{-1} corresponding to aromatic C-H stretch vibrations. The peak at 1643 cm^{-1} is due to -C=N ring stretching and the peak at 1700 cm^{-1} is attributed to C-O stretching vibration in the cyclic hydrocarbons [33]. In the spectrum of the placebo layer we observed two strong peaks at 2880 cm^{-1} and 3440 cm^{-1} bonds corresponding to C-H stretching and O-H stretching vibration, respectively. In the case of the spectrum of the caffeine containing layer, the main peaks of the placebo layer components can also be observed, a broad peak at 3440cm^{-1} and a peak at 2800 cm^{-1}. Interestingly, the main peaks of caffeine cited above are also seen, but with a stronger relative intensity and shift towards higher wavenumbers of the caffeine band at 1640 cm^{-1}. The latter could be associated to some potential interactions between the caffeine and the excipients in the active layer.

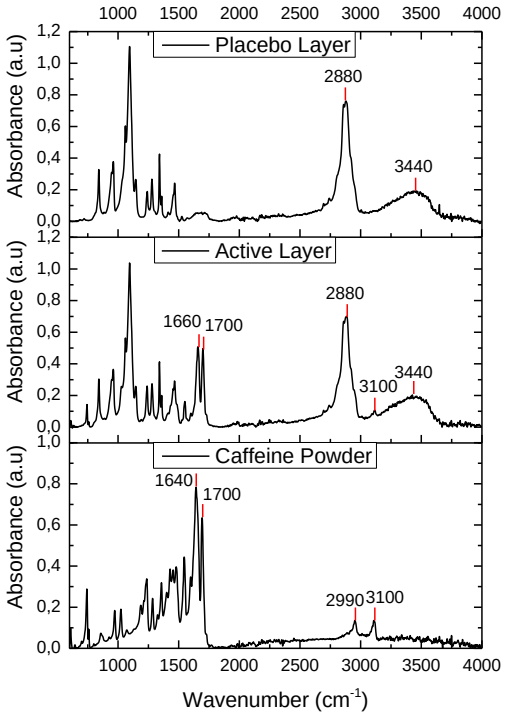

Figure 4. FTIR spectra of caffeine powder, active layer (PEO_CAF_PEG_OA) and placebo layer (PEO _PEG_OA).

 doi:10.20944/preprints202503.2249.v1

3.4. Differential Scanning Calorimetry (DSC)

The selected PEO_CAF_PEG_OA active layer and its placebo counterpart were further analyzed to elucidate the physical states of caffeine and the polymer matrix. Figure 5 presents the DSC thermograms of the active layer, the placebo layer (without caffeine), and pure caffeine powder. The thermogram of pure caffeine exhibited an endothermic peak around 236 °C, corresponding to the melting of caffeine crystals. The placebo electrospun PEO_PEG_OA layer displayed a distinct endothermic peak at 61.96 °C with an enthalpy of fusion of 211.43 J/g (normalized to the mass of the PEO in the layer), associated with the melting characteristics of the PEO crystals. Similarly, the caffeine-loaded fibers showed a PEO melting point at 58.54 °C with an enthalpy of fusion of 205 J/g (normalized to the mass of PEO in the layer). A small decrease in melting point could be associated to the presence of the caffeine that does however not seem to impair the polymer crystallization significantly. Interestingly, the melting peak of caffeine was absent in the thermogram of the caffeine-loaded layer. This absence may be attributed to the electrospinning process inducing a high degree of amorphization of the caffeine within the fibers that does not contribute to a measurable coherent calorimetric signal. Alternatively, since the melting point of caffeine is much higher than the one of PEO, it is possible that any potential caffeine crystals could dissolve in the molten PEO during the DSC run. Thus, to further investigate the physical state of the drug, WAXS experiments were also conducted on the active layer [29].

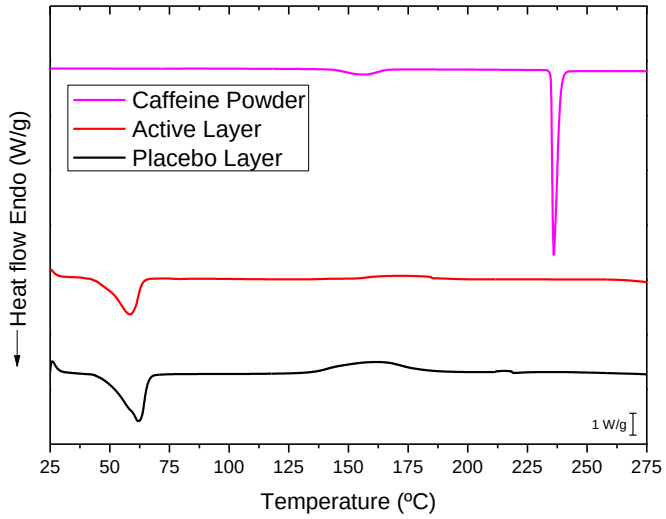

Figure 5. Typical DSC thermograms of caffeine powder, active layer (PEO_CAF_PEG_OA) and placebo layer (PEO _PEG_OA).

3.5. Wide-Angle X-Ray Scattering (WAXS)

The WAXS patterns of the caffeine commercial powder, the PEO_CAF_PEG_OA selected active layer and the PEO_PEG_OA placebo fiber layer were analyzed to assess the potential crystalline structure of the materials. Figure 6 shows the diffractograms of the cited samples. The placebo layer showed two main peaks at 19.2° and 23.5° attributed to the orthorhombic phase of PEO. The caffeine powder diffractogram showed several sharp peaks, attributed to the crystalline nature of the supplied drug. The most intense diffraction peak is observed at 11.6°, which is attributed to the (001) crystalline plane, and two other intense crystalline peaks are present at 26.2° and 26.8°, which are clearly ascribed to the most thermodynamically stable polymorph of caffeine, i.e. the β form [34]. In the case of the PEO_CAF_PEG_OA active layer, the peaks corresponding to the orthorhombic phase of PEO are clearly present at the same diffraction angles (19.2° and 23.5°). Interestingly, another peak is observed at 12.0°, which can only be ascribed to caffeine. This observation suggests that although no endothermic signal was seen by DSC, some crystals of caffeine seem to have been formed within

 doi:10.20944/preprints202503.2249.v1

the fibers during the process. By applying the Scherrer Equation (1) to the only diffraction peak of caffeine seen at ca. 11.6°, the estimated average crystal size for the as received powder is around 20 nm, whereas for the active layer is around 25 nm. So, it appears that within the fibers of the active layer, there exist some very small crystals of caffeine highly dispersed and distributed along the fiber mat, which were not seen as for other compositions of the active layer by SEM on the fibre morphology nor by DSC.

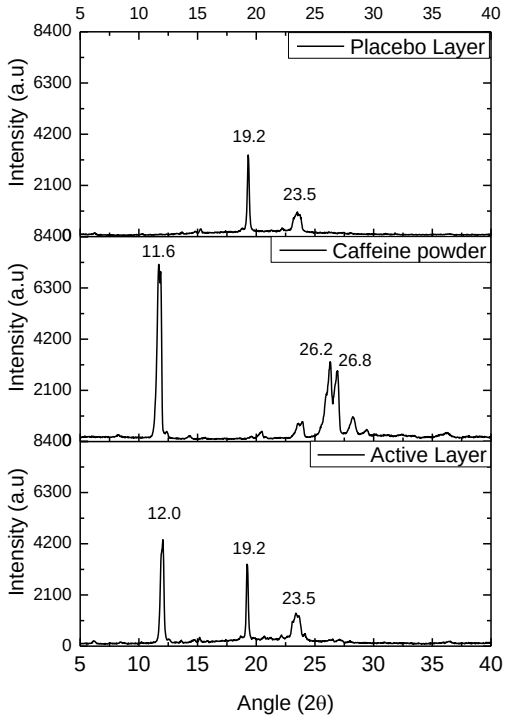

Figure 6. WAXS spectra of caffeine powder, the PEO_CAF_PEG_OA active layer and the PEO_PEG_OA placebo layer.

3.6. Ex-Vivo Human SC Permeation and Modelling of Caffeine

The *ex-vivo* human SC permeation curves can be seen in Figure 7. In this study, we observe that the variation between specimens is higher than with the synthetic membrane, especially at longer testing times, most likely due to the small size of SC tested in the Franz cell equipment, i.e. 1 cm^2. Small skin samples could offer statistically relevant different morphological features between donors such as variable density of hair follicles. Additionally, SC specimens may also undergo variable aging with increasing testing time. In addition, Figure 7 shows that the permeation profile through SC exhibits a different average permeation profile compared to the synthetic membrane, the latter being more bursty at shorter times. The average caffeine permeated after 24 hours provides a value of around 19%, i.e. 0.38 mg/cm^2, of the initial caffeine in the patch, if all four specimens, two from each of the two donors, are considered. Figure 7 also shows that one specimen from the male donor exhibited a comparatively high permeability while for the other three, the caffeine permeation was lower. Abd, Eman et al. reported average caffeine permeability fluxes through human SC for high to very high concentrations of caffeine solutions, i.e. 31.3 mg/mL to 81.5 mg/mL, of 2.2 $\mu g/cm^2$ hour and 25.6 $\mu g/cm^2$ hour, respectively [35]. From this study, a permeation of 0.05 mg/cm^2 and 0.61 mg/cm^2 can be inferred after 24 hours. The authors reported also significant increases in permeation but also in variability among specimens when using enhancers such as OA.

 doi:10.20944/preprints202503.2249.v1

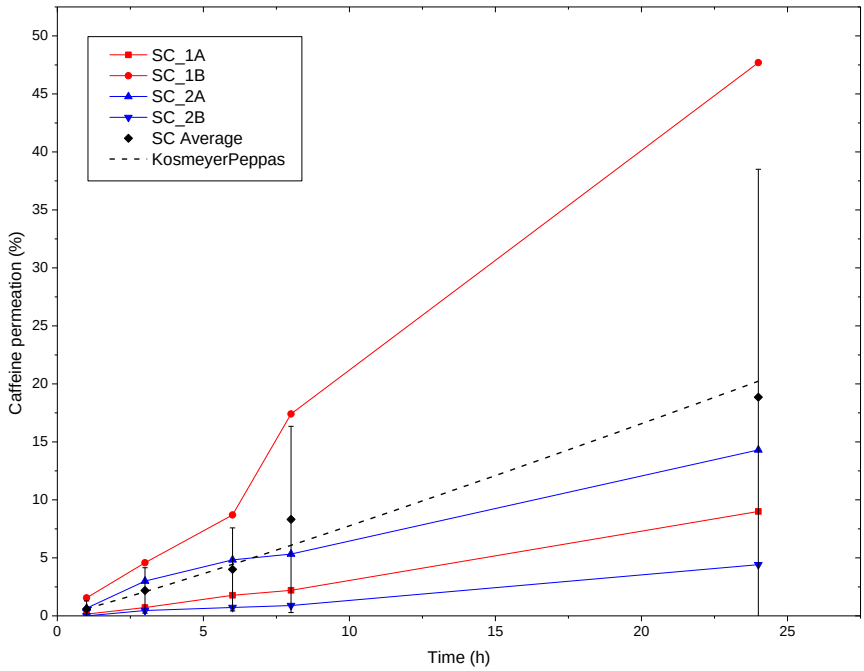

Figure 7. Caffeine permeation through ex-vivo human SC specimens of the PEO_CAF_PEG_OA patch. SC-1A and B correspond to SC specimens of the 39-year-old man and SC-2A and B correspond to SC specimens of the 68-year-old woman. SC Average correspond to the average of all specimens and the dotted line correspond to its fitting to the Kosmeyer-Peppas model.

The modeling of the kinetics of permeation in Figure 7 was fitted with the Korsmeyer-Peppas model (Equation 2), which provided a relatively good regression coefficient value (r^2) (see Table 5). The fitting provides an n value slightly higher than 1. When fitting to the Korsmeyer-Peppas model, an n>1 indicates a clearly non-Fickian permeation process, dominated by significant swelling, erosion, or hydration effects. This behavior is consistent with the PEO nanofibers undergoing considerable swelling and gelling during the release of caffeine.

Table 5. Model parameters of the caffeine permeation profiles of the PEO_CAF_PEG_OA patch through human SC obtained from application of the Korsmeyer-Peppas model.

ID	Korsmeyer-Peppas		
	K	n	r^2
PEO_CAF_PEG_OA patch	0.63	1.09	0.96

4. Conclusions

This study demonstrates the feasibility of the electrospinning technology for generating an innovative bilayer platform for the transdermal delivery of drugs, using caffeine as the model compound. As anticipated, the use of specific enhancers compatible with both the drug and skin composition was confirmed to optimize transdermal delivery. The results indicated that patches containing both polyethylene glycol (PEG) and oleic acid (OA) as enhancers exhibited the highest synergistic effect on caffeine permeability when tested with an artificial membrane. The latter sample was further assessed in transdermal assays using ex vivo human SC specimens as the membrane. The best-performing platform achieved average drug permeation rates of 0.73 mg/cm² in the synthetic membrane after 24 hours.

Notably, it was observed that small crystals of caffeine, averaging 25 nm in size, may have formed during the electrospinning process, which typically yields highly amorphous solid solutions or

 doi:10.20944/preprints202503.2249.v1

dispersions. Further studies are underway to investigate this unusual behavior and to ascertain the extent to which the enhancers may act as nucleants for this and other active pharmaceutical ingredients (API).

Acknowledgements: This research was funded by the Valencian Innovation Agency BIOENCAP project (reference number INNCAD00-18-31), the H2020 EU projects FODIAC (reference number 778388), CAPSULTEK (reference number 873827) and BIOINICIA's internal project ASO PHARM. The authors would also like to thank the experimental assistance provided by Danae Gonzalez-Ortiz from Bionanopharma SL and the Biobank of the Valencia Region for providing the human skin biopsy samples.

References

1. Ramadon, D.; McCrudden, M.T.C.; Courtenay, A.J.; Donnelly, R.F. Enhancement strategies for transdermal drug delivery systems: current trends and applications. *Drug Deliv. Transl. Res.* **2022**, *12*, 758–791, doi:10.1007/s13346-021-00909-6.
2. Shi, Y.; Xu, S.; Dong, A. Design and in vitro evaluation of transdermal patches based on ibuprofen-loaded electrospun fiber mats. **2013**, 333–341, doi:10.1007/s10856-012-4805-1.
3. Trommer, H.; Neubert, R.H.H. Overcoming the stratum corneum: The modulation of skin penetration. A review. *Skin Pharmacol. Physiol.* **2006**, *19*, 106–121, doi:10.1159/000091978.
4. van Smeden, J.; Janssens, M.; Gooris, G.S.; Bouwstra, J.A. The important role of stratum corneum lipids for the cutaneous barrier function. *Biochim. Biophys. Acta - Mol. Cell Biol. Lipids* **2014**, *1841*, 295–313, doi:10.1016/j.bbalip.2013.11.006.
5. Moghadam, S.H.; Saliaj, E.; Wettig, S.D.; Dong, C.; Ivanova, M. V; Huzil, J.T.; Foldvari, M. Effect of Chemical Permeation Enhancers on Stratum Corneum.pdf. **2013**.
6. Prausnitz, M.R.; Langer, R. Transdermal drug delivery. *Nat. Biotechnol.* **2008**, *26*, 1261–1268, doi:10.1038/nbt.1504.
7. Kováčik, A.; Kopečná, M.; Vávrová, K. Permeation enhancers in transdermal drug delivery: benefits and limitations. *Expert Opin. Drug Deliv.* **2020**, *17*, 145–155, doi:10.1080/17425247.2020.1713087.
8. Dragicevic, N.; Maibach, H.I. Percutaneous penetration enhancers chemical methods in penetration enhancement: Modification of the stratum corneum. *Percutaneous Penetration Enhanc. Chem. Methods Penetration Enhanc. Modif. Strat. Corneum* **2015**, 1–411, doi:10.1007/978-3-662-47039-8.
9. Arellano, A.; Santoyo, S.; Martn, C.; Ygartua, P. Surfactant effects on the in vitro percutaneous absorption of diclofenac sodium. *Eur. J. Drug Metab. Pharmacokinet.* **1998**, *23*, 307–312, doi:10.1007/BF03189356.
10. Ibrahim, M.M.A.; Sammour, O.A.; Hammad, M.A.; Megrab, N.A. In vitro evaluation of proniosomes as a drug carrier for flurbiprofen. *AAPS PharmSciTech* **2008**, *9*, 782–790, doi:10.1208/s12249-008-9114-0.
11. Xu, W.; Liu, C.; Zhang, Y.; Quan, P.; Yang, D.; Fang, L. An investigation on the effect of drug physicochemical properties on the enhancement strength of enhancer: The role of drug-skin-enhancer interactions. *Int. J. Pharm.* **2021**, *607*, 120945, doi:10.1016/j.ijpharm.2021.120945.
12. Schulz, M.; Fussnegger, B.; Bodmeier, R. Drug release and adhesive properties of crospovidone-containing matrix patches based on polyisobutene and acrylic adhesives. *Eur. J. Pharm. Sci.* **2010**, *41*, 675–684, doi:10.1016/j.ejps.2010.09.011.
13. Teno, J.; Pardo-Figuerez, M.; Figueroa-Lopez, K.J.; Prieto, C.; Lagaron, J.M. Development of Multilayer Ciprofloxacin Hydrochloride Electrospun Patches for Buccal Drug Delivery. *J. Funct. Biomater.* **2022**, *13*, 170, doi:10.3390/jfb13040170.
14. Pardo-Figuerez, M.; Teno, J.; Lafraya, A.; Prieto, C.; Lagaron, J.M. Development of an Electrospun Patch Platform Technology for the Delivery of Carvedilol in the Oral Mucosa. *Nanomaterials* **2022**, *12*, 438, doi:10.3390/nano12030438.
15. Patel, M.; Patel, A.; Desai, J.; Patel, S. Cutaneous Pharmacokinetics of Topically Applied Novel Dermatological Formulations. *AAPS PharmSciTech* **2024**, *25*, 1–18, doi:10.1208/s12249-024-02763-4.
16. Kushwaha, R.; Palei, N.N. Transdermal Drug Delivery Systems: Different Generations and Dermatokinetic Assessment of Drug Concentration in Skin. *Pharmaceut. Med.* **2024**, *38*, 407–427, doi:10.1007/s40290-024-00537-8.
17. Gaydhane, M.K.; Sharma, C.S.; Majumdar, S. Electrospun nanofibres in drug delivery: advances in controlled release strategies. *RSC Adv.* **2023**, *13*, 7312–7328, doi:10.1039/D2RA06023J.

 doi:10.20944/preprints202503.2249.v1

18. Dziemidowicz, K.; Sang, Q.; Wu, J.; Zhang, Z.; Zhou, F.; Lagaron, J.M.; Mo, X.; Parker, G.J.M.; Yu, D.G.; Zhu, L.M.; et al. Electrospinning for healthcare: recent advancements. *J. Mater. Chem. B* **2021**, *9*, 939–951, doi:10.1039/d0tb02124e.
19. Yu, D.G.; Shen, X.X.; Branford-White, C.; White, K.; Zhu, L.M.; Annie Bligh, S.W. Oral fast-dissolving drug delivery membranes prepared from electrospun polyvinylpyrrolidone ultrafine fibers. *Nanotechnology* **2009**, *20*, doi:10.1088/0957-4484/20/5/055104.
20. Joiner, J.B.; Prasher, A.; Young, I.C.; Kim, J.; Shrivastava, R.; Maturavongsadit, P.; Benhabbour, S.R. Effects of Drug Physicochemical Properties on In-Situ Forming Implant Polymer Degradation and Drug Release Kinetics. *Pharmaceutics* **2022**, *14*, doi:10.3390/pharmaceutics14061188.
21. Luraghi, A.; Peri, F.; Moroni, L. Electrospinning for drug delivery applications: A review. *J. Control. Release* **2021**, *334*, 463–484, doi:10.1016/j.jconrel.2021.03.033.
22. Pant, B.; Park, M.; Park, S.J. Drug delivery applications of core-sheath nanofibers prepared by coaxial electrospinning: A review. *Pharmaceutics* **2019**, *11*, doi:10.3390/pharmaceutics11070305.
23. Weiser, T.W. Caffeine as analgesic adjuvant. In *Treatments, mechanisms, and adverse reactions of anesthetics and analgesics*; Elsevier, 2022; pp. 63–72.
24. Sumedha, V.; Shiva, S.; Manikantan, S.; Ramakrishna, S. European Journal of Medicinal Chemistry Reports Pharmacology of caffeine and its effects on the human body. *Eur. J. Med. Chem. Reports* **2024**, *10*, 100138, doi:10.1016/j.ejmcr.2024.100138.
25. Visconti, M.J.; Haidari, W.; Feldman, S.R. Therapeutic use of caffeine in dermatology: A literature review. *J. Dermatology Dermatologic Surg.* **2020**, *24*, 18–24, doi:10.4103/jdds.jdds_52_19.
26. Herman, A.; Herman, A.P. Caffeine's mechanisms of action and its cosmetic use. *Skin Pharmacol. Physiol.* **2012**, *26*, 8–14, doi:10.1159/000343174.
27. Avizheh, L.; Peirouvi, T.; Diba, K.; Fathi-Azarbayjani, A. Electrospun wound dressing as a promising tool for the therapeutic delivery of ascorbic acid and caffeine. *Ther. Deliv.* **2019**, *10*, 757–767, doi:10.4155/tde-2019-0059.
28. Li, X.; Kanjwal, M.A.; Lin, L.; Chronakis, I.S. Electrospun polyvinyl-alcohol nanofibers as oral fast-dissolving delivery system of caffeine and riboflavin. *Colloids Surfaces B Biointerfaces* **2013**, *103*, 182–188, doi:10.1016/j.colsurfb.2012.10.016.
29. Illangakoon, U.E.; Gill, H.; Shearman, G.C.; Parhizkar, M.; Mahalingam, S.; Chatterton, N.P.; Williams, G.R. Fast dissolving paracetamol/caffeine nanofibers prepared by electrospinning. *Int. J. Pharm.* **2014**, *477*, 369–379, doi:10.1016/j.ijpharm.2014.10.036.
30. Mathematical models of drug release. In *Strategies to Modify the Drug Release from Pharmaceutical Systems*; Elsevier, 2015; pp. 63–86 ISBN 9780081000922.
31. Seif, S.; Franzen, L.; Windbergs, M. Overcoming drug crystallization in electrospun fibers - Elucidating key parameters and developing strategies for drug delivery. *Int. J. Pharm.* **2015**, *478*, 390–397, doi:10.1016/j.ijpharm.2014.11.045.
32. Naik, A.; Pechtold, L.A.R.M.; Potts, R.O.; Guy, R.H. Mechanism of oleic acid-induced skin penetration enhancement in vivo in humans. *J. Control. Release* **1995**, *37*, 299–306, doi:10.1016/0168-3659(95)00088-7.
33. Silvertein, R.M.; Webster, F.X.; Kiemle, D.. *Silverstein - Spectrometric Identification of Organic Compounds*; Wiley, Ed.; 7th ed.; **2005**; ISBN 0-471-39365-2.
34. Sarfraz, A.; Simo, A.; Fenger, R.; Christen, W.; Rademann, K.; Panne, U.; Emmerling, F. Morphological Diversity of Caffeine on Surfaces : Needles and Hexagons Published as part of a virtual special issue of selected papers presented at the 2010 Annual Conference of the. *Cryst. Growth Des.* **2011**, 583–588.
35. Eman, A.; Namjoshi, S.; Mohammed, Y.; Roberts, M.S.; Grice, J.E.. Synergistic Skin Penetration Enhancer and Nanoemulsion Formulations Promote the Human Epidermal Permeation of Caffeine and Naproxen. *Journal of Pharmaceutical Sciences*, **2016**, Volume 105, Issue 1, 212 – 220.